DALTON
FULL PAPER

Supramolecular organization in *catena*-poly{diethyl[3-(2-pyridyl)-2-sulfanylpropenoato]tin(IV)} and related diorganotin(IV) sulfanylcarboxylato compounds

José S. Casas,[a] Alfonso Castiñeiras,[a] Maria D. Couce,[b] Nuria Playá,[a] Umberto Russo,[c] Agustin Sánchez,[a] José Sordo *,[a] and José Mª Varela [a]

[a] *Departamento de Química Inorgánica, Facultade de Farmacia, Universidade de Santiago de Compostela, 15706 Santiago de Compostela, Spain*
[b] *Departamento de Química Pura e Aplicada, Facultade de Ciencias, Universidade de Vigo, 36200 Vigo, Spain*
[c] *Dipartimento di Chimica Inorganica, Metallorganica ed Analitica, Universita di Padova, Via Marzolo 1, 35100 Padova, Italy*

Reaction of 3-(2-aryl)-2-sulfanylpropenoic acids with diorganotin(IV) oxides afforded compounds of the type [SnR_2L] [R = Me, Et, Bu^n or Ph; H_2L = 3-(2-thienyl)-, -(phenyl)- or -(2-pyridyl)-2-sulfanylpropenoic acid]. The structure of [$SnEt_2$(pyspa)] was determined by single-crystal X-ray diffraction and shown to be polymeric, with the tin atom in a distorted trigonal-bipyramidal environment created by intramolecular bonds to a C atom of each of two ethyl groups and to a sulfur and a carboxylic oxygen of the pyspa ligand together with an additional intermolecular Sn–O bond. Mass, Mössbauer, IR, Raman and NMR spectroscopy of the other eleven compounds prepared suggests similar polymeric structures for all.

Organotin compounds in biological media react with thiol groups of biologically relevant molecules, yielding products characterized by Sn–S bonds.[1] This fact has led to considerable effort being devoted to characterizing model compounds obtained from ligands which have a second donor atom or group as well as a thiol group.[2] A biologically interesting second donor is the carboxylato group, which coexists with the thiol group in several biologically relevant species, such as amino acids and glutathione (γ-glutamylcysteinylglycine). The interaction of sulfanylcarboxylate ligands with organotin(IV) compounds is also interesting industrially, since some diorganotin sulfanylcarboxylato complexes are widely used as polyvinyl chloride stabilizers.[3]

Although several organotin sulfanylcarboxylato complexes have been prepared and characterized spectroscopically,[4] structural studies based on X-ray diffraction have as far as we know been limited to two cyclic di-*n*-butyltin hexamers, the 3-sulfanylpropionate[5] and the thiosalicylate.[6] Since the complexes of 3-aryl-2-sulfanylpropenoic acids with metal ions are more stable than those of the corresponding 3-aryl-2-sulfanylpropanoic acids, and since some are soluble in organic solvents[7] (which can facilitate crystallization), in this work we studied the dimethyl-, diethyl-, di-*n*-butyl- and diphenyl-tin(IV) complexes of three sulfanylpropenoic acids with five- or six-membered rings, namely 2-thienyl- (t), phenyl- (p) and 2-pyridyl- (py) sulfanylpropenoic acids (Scheme 1). Note that in H_2pyspa both the ring and the mpa moiety have potential donor atoms. This paper describes the preparation and spectroscopic characterization of these compounds and the crystal structure of diethyl[3-(2-pyridyl)-2-sulfanylpropenoato]tin(IV), which differs from the two previously known organotin sulfanylcarboxylate structures in being polymeric.

Experimental

Material and methods

3-(2-Aryl)-2-sulfanylpropenoic acids were prepared[8] by condensation of the appropriate aldehyde with rhodanine, subsequent hydrolysis in an alkaline medium and acidification with aqueous HCl. Dimethyltin oxide (Johnson Matthey) and dibutyltin oxide (Aldrich-Chemie) were used as supplied. Diethyltin and diphenyltin oxides were obtained by treating diethyl- and diphenyl-tin dichloride with sodium hydroxide. Elemental analyses were performed with a Carlo-Erba 1108 apparatus. Melting points were determined using a Büchi apparatus. Mössbauer spectra were determined at 80.0 K, unless otherwise stated, in a constant-acceleration apparatus with a $Ca^{119m}SnO_3$ source, and were referred to SnO_2; to minimize preferential crystallite orientations or texture effects the samples were ground to a fine powder and dispersed uniformly in vaseline. The IR spectra were recorded in KBr discs or Nujol mulls on a Bruker IFS 66v FT-IR spectrometer, and Raman spectra of polycrystalline samples were recorded on the same spectrometer using an FRA-106 accessory (v = very, s = strong, m = medium, w = weak). Proton and ^{13}C NMR spectra were obtained in $(CD_3)_2SO$ at room temperature on Bruker AMX300 or AMX500 spectrometers and referenced to $SiMe_4$. Mass spectra were recorded on a Kratos MS50TC spectrometer connected to a DS90 data system and operating under FAB conditions [Xe, 8 eV (*ca.* 1.28×10^{-15} J)]; the matrix used is described in each case. Conductivities (dmso, 10^{-3} M) were determined with a WTW-LF3 conductivity meter.

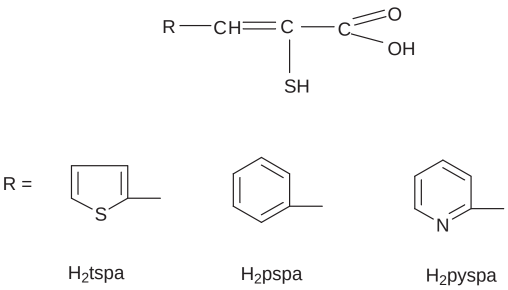

Scheme 1

Preparations

The compounds were prepared by adding the SnR_2O oxide to a solution of the appropriate sulfanylcarboxylic acid in ethanol. After stirring at room temperature the solid formed was filtered off and vacuum dried.

[SnMe$_2$(tspa)]. SnMe$_2$O (0.41 g, 2.5 mmol), H$_2$tspa (0.47 g, 2.5 mmol), ethanol (45 cm^3), 5 d stirring, yellow solid. Yield: 95%. M.p. >300 °C (Found: C, 32.8; H, 3.0; S, 19.5. Calc. for $C_9H_{10}O_2S_2Sn$: C, 32.5; H, 3.0; S, 19.4%). IR and Raman (R) (cm^{-1}): $\nu_{asym}(CO_2)$ 1525vs (IR); $\nu_{sym}(CO_2)$ 1373vs (IR), 1368m (R); ν_{asym}(Sn–C) 574m (IR), 570w (R); ν_{sym}(Sn–C) 528m (IR), 530m (R); ν(Sn–S) 349m (IR), 348w (R). Mass spectrum (*m*-nitrobenzyl alcohol): *m*/*z* 335 ($[M + H]^+$ 4.1) and 667 ($[2M - H]^+$, 1.5%). Mössbauer: δ 1.35, ΔE_Q 3.12, Γ 0.97 mm s^{-1}, $A_{2/1}$ 0.95. Λ_M 0.9 S cm^2 mol^{-1}.

[SnEt$_2$(tspa)]. SnEt$_2$O (0.65 g, 3.4 mmol), H$_2$tspa (0.63 g, 3.4 mmol), ethanol (60 cm^3), 4 d stirring, beige solid. Yield: 89%. M.p. >300 °C (Found: C, 36.3; H, 3.9; S, 16.7. Calc. for $C_{11}H_{14}O_2S_2Sn$: C, 36.6; H, 3.9; S, 17.3%). IR and Raman (R) (cm^{-1}): $\nu_{asym}(CO_2)$ 1520vs; $\nu_{sym}(CO_2)$ 1370vs (IR), 1367m (R); ν_{asym}(Sn–C) 525m (IR), 533w (R); ν_{sym}(Sn–C) 505m (IR), 503m (R); ν(Sn–S) 347m (IR), 348w (R). Mass spectrum [*m*-nitrobenzyl alcohol–bis(2-hydroxyethyl) disulfide]: *m*/*z* 363 ($[M + H]^+$, 2.6%). Mössbauer: δ 1.44, ΔE_Q 3.13, Γ 0.97 mm s^{-1}, $A_{2/1}$ 0.98. Λ_M 0.6 S cm^2 mol^{-1}.

[SnBu$_2$(tspa)]. SnBu$_2$O (0.67 g, 2.7 mmol), H$_2$tspa (0.50 g, 2.7 mmol), ethanol (50 cm^3), 4 d stirring, yellow solid. Yield: 77%. M.p. 215 °C (Found: C, 43.7; H, 5.1; S, 15.4. Calc. for $C_{15}H_{22}O_2S_2Sn$: C, 43.2; H, 5.3; S, 15.4%). IR and Raman (R) (cm^{-1}): $\nu_{asym}(CO_2)$ 1522vs; $\nu_{sym}(CO_2)$ 1373vs (IR), 1371m (R); ν_{asym}(Sn–C) 654m (IR), 653w (R); ν_{sym}(Sn–C) 606m (IR), 606w (R); ν(Sn–S) 350 (sh) (IR), 349w (R). Mass spectrum (*m*-nitrobenzyl alcohol): *m*/*z* 177, (SnBu), (68.6), 305 ($[M - 2Bu + H]^+$, 41.5), 419 ($[M + H]^+$, 100.0) and 1251 ($[3M - 3H]^+$, 0.5%). Mössbauer: δ 1.45, ΔE_Q 3.15, Γ 0.88 mm s^{-1}, $A_{2/1}$ 1.04. Λ_M 0.7 S cm^2 mol^{-1}.

[SnPh$_2$(tspa)]. SnPh$_2$O (0.52 g, 1.8 mmol), H$_2$tspa (0.34 g, 1.8 mmol), ethanol (50 cm^3), 4 d stirring, beige solid. Yield: 80%. M.p. >300 °C (Found: C, 49.5; H, 3.0; S, 14.7. Calc. for $C_{19}H_{14}O_2S_2Sn$: C, 49.9; H, 3.1; S, 14.0%). IR and Raman (R) (cm^{-1}): $\nu_{asym}(CO_2)$ 1522vs (IR); $\nu_{sym}(CO_2)$ 1370vs (IR), 1366m (R); ν_{asym}(Sn–C) 280m (IR), 288w (R); ν_{sym}(Sn–C) 231m (IR), 225w (R); ν(Sn–S) 360m (IR), 358w (R). Mass spectrum [*m*-nitrobenzyl alcohol–bis(2-hydroxyethyl) disulfide]: *m*/*z* 459 ($[M + H]^+$, 2.2%). Mössbauer: δ 1.30, ΔE_Q 3.11, Γ 0.89 mm s^{-1}, $A_{2/1}$ 1.01. Λ_M 0.6 S cm^2 mol^{-1}.

[SnMe$_2$(pspa)]. SnMe$_2$O (0.64 g, 3.9 mmol), H$_2$pspa (0.70 g, 3.9 mmol), ethanol (50 cm^3), 4 d stirring, beige solid. Yield: 82%. M.p. >300 °C (Found: C, 41.2; H, 3.7; S, 10.0. Calc. for $C_{11}H_{12}O_2SSn$: C, 41.4; H, 3.7; S, 9.8%). IR and Raman (R) (cm^{-1}): $\nu_{asym}(CO_2)$ 1530vs (IR); $\nu_{sym}(CO_2)$ 1373vs (IR), 1368m (R); ν_{asym}(Sn–C) 565m (IR), 567w (R); ν_{sym}(Sn–C) 529s (IR), 531m (R); ν(Sn–S) 357m (IR), 354w (R). Mass spectrum (*m*-nitrobenzyl alcohol): *m*/*z* 329 ($[M + H]^+$, 12.1) and 655 ($[2M - H]^+$, 2.3%). Mössbauer: δ 1.35, ΔE_Q 3.16, Γ 0.87 mm s^{-1}, $A_{2/1}$ 1.03. Λ_M 0.9 S cm^2 mol^{-1}.

[SnEt$_2$(pspa)]. SnEt$_2$O (0.65 g, 3.4 mmol), H$_2$pspa (0.61 g, 3.4 mmol), ethanol (50 cm^3), 4 d stirring, beige solid. Yield: 89%. M.p. 290 °C (Found: C, 43.9; H, 4.5; S, 9.0. Calc. for $C_{13}H_{16}O_2SSn$: C, 44.0; H, 4.5; S, 9.0%). IR and Raman (R) (cm^{-1}): $\nu_{asym}(CO_2)$ 1522vs (IR); $\nu_{sym}(CO_2)$ 1372vs (IR), 1366m (R); ν_{asym}(Sn–C) 525s (IR), 520w (R); ν_{sym}(Sn–C) 507m (IR), 506m (R); ν(Sn–S) 357m (IR), 354w (R). Mass spectrum (*m*-nitrobenzyl alcohol): *m*/*z* 355 (*M*, 9.9) and 711 ($[2M + H]^+$, 2.4%). Mössbauer: δ 1.46, ΔE_Q 3.24, Γ 0.88 mm s^{-1}, $A_{2/1}$ 0.99. Λ_M 0.7 S cm^2 mol^{-1}.

[SnBu$_2$(pspa)]. SnBu$_2$O (1.11 g, 4.4 mmol), H$_2$pspa (0.80 g, 4.4 mmol), ethanol (50 cm^3), 3 d stirring, white solid. Yield: 89%. M.p. 190 °C (Found: C, 48.8; H, 5.8; S, 6.7. Calc. for $C_{17}H_{24}O_2SSn$: C, 49.7; H, 5.9; S, 7.8%). IR and Raman (R) (cm^{-1}): $\nu_{asym}(CO_2)$ 1523vs (IR); $\nu_{sym}(CO_2)$ 1375vs (IR), 1370m (R); ν_{asym}(Sn–C) 635w (IR); ν_{sym}(Sn–C) 599w (IR), 596w (R); ν(Sn–S) 355m (IR), 354w (R). Mass spectrum (*m*-nitrobenzyl alcohol): *m*/*z* 177 ([Sn + Bu], 70.7), 413 ($[M + H]^+$ 100.0), 1175 ($[3M - Bu - 4H]^+$, 1.9) and 1233 ($[3M - 3H]^+$, 0.7%). Mössbauer: δ 1.45, ΔE_Q 3.16, Γ 0.92 mm s^{-1}, $A_{2/1}$ 1.05. Λ_M 0.7 S cm^2 mol^{-1}.

[SnPh$_2$(pspa)]. SnPh$_2$O (0.34 g, 1.2 mmol), H$_2$pspa (0.22 g, 1.2 mmol), ethanol (50 cm^3), 4 d stirring, white solid. Yield: 56%. M.p. >300 °C (Found: C, 55.4; H, 3.4; S, 6.7. Calc. for $C_{21}H_{16}O_2SSn$: C, 55.9; H, 3.6; S, 7.1%). IR and Raman (R) (cm^{-1}): $\nu_{asym}(CO_2)$ 1525vs (IR); $\nu_{sym}(CO_2)$ 1371vs (IR), 1365m (R); ν_{asym}(Sn–C) 285m (IR), 279w (R); ν_{sym}(Sn–C) 222m (IR), 221w (R); ν(Sn–S) 366m (IR), 367w (R). Mass spectrum [bis(2-hydroxyethyl disulfide]: *m*/*z* 453 ($[M + H]^+$, 0.6%). Mössbauer: δ 1.29, ΔE_Q 3.09, Γ 0.89 mm s^{-1}, $A_{2/1}$ 1.02. Λ_M 1.2 S cm^2 mol^{-1}.

[SnMe$_2$(pyspa)]. SnMe$_2$O (0.73 g, 4.4 mmol), H$_2$pyspa (0.80 g, 4.4 mmol), ethanol (50 cm^3), 2 d stirring, brown solid. Yield: 75%. M.p. 290 °C (Found: C, 36.3; H, 3.5; N, 4.2; S, 9.4. Calc. for $C_9H_{11}NO_2SSn$: C, 36.6; H, 3.4; N, 4.3; S, 9.8%). IR and Raman (R) (cm^{-1}): $\nu_{asym}(CO_2)$ 1555vs (IR); $\nu_{sym}(CO_2)$ 1373vs (IR), 1370m (R); ν_{asym}(Sn–C) 567m (IR); ν_{sym}(Sn–C) 528s (IR), 532m (R); ν(Sn–S) 364m (IR), 364w (R). Mass spectrum (thioglycerol): *m*/*z* 330 ($[M + H]^+$, 96.2%). Mössbauer: δ 1.35, ΔE_Q 3.13, Γ 0.90 mm s^{-1}, $A_{2/1}$ 0.97. Λ_M 1.1 S cm^2 mol^{-1}.

[SnEt$_2$(pyspa)]. SnEt$_2$O (0.50 g, 2.6 mmol), H$_2$pyspa (0.47 g, 2.6 mmol), ethanol (50 cm^3), 5 d stirring, orange-brown solid. Yield: 83%. M.p. 285 °C (Found: C, 40.2; H, 4.3; N, 3.8; S, 9.0. Calc. for $C_{12}H_{15}NO_2SSn$: C, 40.5; H, 4.25; N, 3.9; S, 9.0%). IR and Raman (R) (cm^{-1}): $\nu_{asym}(CO_2)$ 1530vs (IR); $\nu_{sym}(CO_2)$ 1371vs (IR), 1370m (R); ν_{asym}(Sn–C) 535m (IR), 535w (R); ν_{sym}(Sn–C) 509m (IR), 506m (R); ν(Sn–S) 362m (IR), 362w (R). Mass spectrum (*m*-nitrobenzyl alcohol): *m*/*z* 358 ($[M + H]^+$, 100.0) and 713 ($[2M - H]^+$, 2.7%). Mössbauer: δ 1.47, ΔE_Q 3.22, Γ 0.90 mm s^{-1}, $A_{2/1}$ 1.04. Λ_M 1.4 S cm^2 mol^{-1}. Recrystallization of this solid from dmso yielded crystals suitable for X-ray analysis.

[SnBu$_2$(pyspa)]. SnBu$_2$O (1.10 g, 4.4 mmol), H$_2$pyspa (0.80 g, 4.4 mmol), ethanol (50 cm^3), 4 d stirring, beige solid. Yield: 75%. M.p. 217 °C (Found: C, 45.9; H, 5.8; N, 3.5; S, 8.3. Calc. for $C_{16}H_{23}NO_2SSn$: C, 46.7; H, 5.6; N, 3.4; S, 7.8%). IR and Raman (R) (cm^{-1}): $\nu_{asym}(CO_2)$ 1531vs (IR); $\nu_{sym}(CO_2)$ 1378vs (IR), 1375m (R); ν_{asym}(Sn–C) 632m (IR), 629w (R); ν_{sym}(Sn–C) 606m (IR), 608w (R); ν(Sn–S) 362m (IR), 363w (R). Mass spectrum (*m*-nitrobenzyl alcohol): *m*/*z* 177 ([Sn + Bu], 6.9), 414 ($[M + H]^+$, 100.0), 825 ($[2M - H]^+$, 2.0) and 1236 ($[3M - 3H]^+$, 0.2%). Mössbauer: δ 1.48, ΔE_Q 3.20, Γ 0.86 mm s^{-1}, $A_{2/1}$ 1.06. Λ_M 0.7 S cm^2 mol^{-1}.

[SnPh$_2$(pyspa)]. SnPh$_2$O (0.30 g, 1.0 mmol), H$_2$pyspa (0.19 g, 1.0 mmol), ethanol (35 cm^3), 5 d stirring, green solid. Yield: 70%. M.p. 280 °C (Found: C, 53.5; H, 3.0; N, 3.0; S, 5.4. Calc. for $C_{20}H_{15}NO_2SSn$: C, 53.1; H, 3.3; N, 3.1; S, 7.1%). IR and Raman (R) (cm^{-1}): $\nu_{asym}(CO_2)$ 1533vs (IR); $\nu_{sym}(CO_2)$ 1373vs (IR); ν_{asym}(Sn–C) 272m (IR); ν_{sym}(Sn–C) 225m (IR); ν(Sn–S) 368m (IR). Mass spectrum (*m*-nitrobenzyl alcohol): *m*/*z* 197 ([SnPh], 33.1), 454 ($[M + H]^+$, 100.0) and 905 ($[2M - H]^+$, 3.5%). Mössbauer: δ 1.29, ΔE_Q 3.02, Γ 0.87 mm s^{-1}, $A_{2/1}$ 0.97. Λ_M 1.5 S cm^2 mol^{-1}.

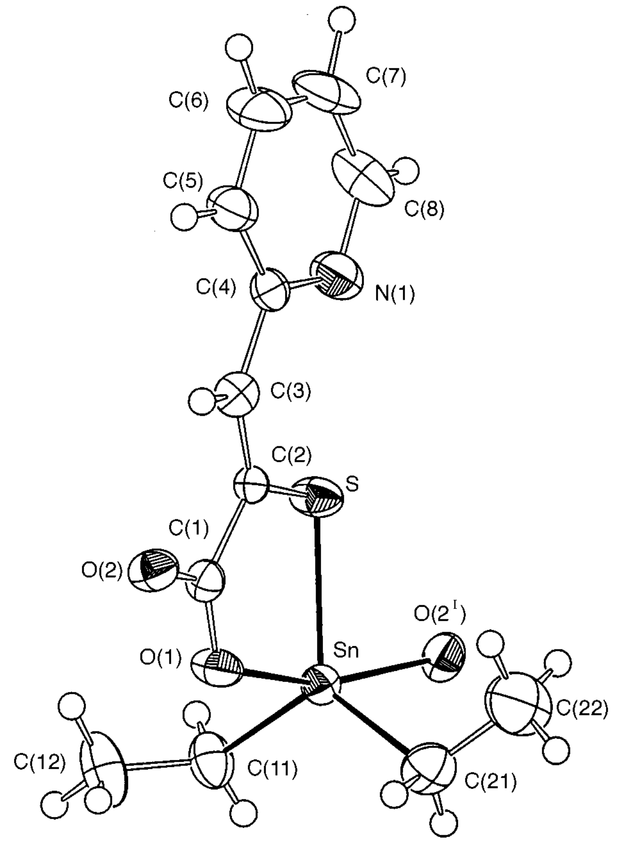

Fig. 1 Crystal structure of [SnEt$_2$(pyspa)], showing the numbering scheme

Table 1 Crystal data and structure refinement for [SnEt$_2$(pyspa)]

Empirical formula	$C_{12}H_{15}NO_2SSn$
M	356.00
T/K	293(2)
Crystal system, space group	Orthorhombic, *Pbca*
a/Å	23.455(4)
b/Å	11.1793(14)
c/Å	10.3097(12)
U/Å^3	2703.3(6)
Z, D_c/Mg m^{-3}	8, 1.749
μ/mm^{-1}	2.043
F(000)	1408
Crystal size/mm	0.30 × 0.20 × 0.15
λ(Mo-Kα)/Å	0.710 73
θ Range for data collection/°	3.20 to 29.94
Index ranges	$0 \leq h \leq 32$, $0 \leq k \leq 15$, $-14 \leq l \leq 0$
Reflections collected/unique	3919/3919[*R*(int) = 0.0000]
Absorption correction	Empirical
Maximum, minimum transmission	0.7501, 0.5805
Data, restraints, parameters	3919, 0, 215
Goodness of fit on F^2	1.008
Final *R*1, *wR*2 [$I > 2\sigma(I)$]	0.0527, 0.0821
(all data)	0.1268, 0.1001
Extinction coefficient	0.000 12(9)
Largest difference peak, hole	0.789, −0.755 e Å^{-3}

Table 2 Selected bond lengths (Å) and angles (°) in [SnEt$_2$(pyspa)]

Sn–S	2.424(2)	O(2)–C(1)	1.271(6)
Sn–O(1)	2.226(4)	C(1)–C(2)	1.503(7)
Sn–O(2^{I})*	2.219(4)	C(2)–C(3)	1.354(8)
Sn–C(11)	2.134(6)	C(3)–C(4)	1.459(8)
Sn–C(21)	2.128(7)	C(11)–C(12)	1.493(10)
S–C(2)	1.742(5)	C(21)–C(22)	1.506(11)
O(1)–C(1)	1.258(6)		
S–Sn–O(1)	79.89(10)	O(1)–C(1)–O(2)	122.0(5)
S–Sn–O(2^{I})	84.96(12)	O(1)–C(1)–C(2)	120.2(5)
S–Sn–C(11)	118.7(3)	O(2)–C(1)–C(2)	117.8(5)
S–Sn–C(21)	118.8(2)	S–C(2)–C(1)	118.1(4)
O(1)–Sn–O(2^{I})	162.51(15)	S–C(2)–C(3)	124.6(4)
O(1)–Sn–C(11)	96.8(2)	C(1)–C(2)–C(3)	117.3(5)
O(1)–Sn–C(21)	90.6(2)	C(2)–C(3)–C(4)	130.6(6)
O(2^{I})–Sn–C(11)	98.2(2)	N(1)–C(4)–C(3)	119.1(6)
O(2^{I})–Sn–C(21)	89.1(2)	N(1)–C(4)–C(5)	121.7(6)
C(11)–Sn–C(21)	122.5(3)	C(3)–C(4)–C(5)	119.1(6)

* $x, -y + \frac{3}{2}, z + \frac{1}{2}$.

Crystallography

X-Ray data collection and reduction. An amber prismatic crystal of [SnEt$_2$(pyspa)] was mounted on a glass fibre for data collection in an Enraf-Nonius CAD4 automatic diffractometer.[9] Cell constants and an orientation matrix for data collection were obtained by least-squares refinement of the diffraction data for 25 reflections in the range $6.7 \leq \theta \leq 12.1°$. Data were collected at 293 K using Mo-Kα radiation (λ = 0.710 73 Å) and the ω–2θ scan technique, and were corrected for Lorentz-polarization effects. An empirical absorption correction was also made.[10] Table 1 summarizes the crystal data, experimental details and refinement results.

Structure solution and refinement. The structure was solved by direct methods,[11] which revealed the positions of all non-hydrogen atoms, and was refined on F^2 by a full-matrix least-squares procedure using anisotropic displacement parameters for all non-hydrogen atoms.[12] Hydrogen atoms were located in the Fourier-difference maps, and refined isotropically. A secondary extinction correction was applied.[12] When all shift/e.s.d. ratios were less than 0.001, the agreement factors were those listed in Table 1. Atomic scattering factors were taken from ref. 13. Molecular graphics were obtained with ZORTEP[14] and SCHAKAL.[15]

CCDC reference number 186/914.

See http://www.rsc.org/suppdata/dt/1998/1513/ for crystallographic files in .cif format.

Results and Discussion

Structure of [SnEt$_2$(pyspa)]

Tin co-ordination sphere. Fig. 1 shows the structure of [SnEt$_2$(pyspa)] and the numbering scheme. Each tin atom is co-ordinated to two ethyl C atoms, to the S atom and O(1) atom of one pyspa carboxylato group, and to the O(2) atom of a neighbouring molecule, giving it a distorted trigonal-bipyramidal environment in which the oxygen atoms are apical.

The Sn–C bond lengths (Table 2) are unremarkable; the Sn–S distance is very close to the sum of the covalent radii of tin and sulfur (2.42 Å).[16] The intra- and inter-molecular Sn–O bond lengths, which are equal to within the e.s.d.s, are slightly greater than the sum of the covalent radii of tin and oxygen, 2.13 Å.[16] The Sn atom is only 0.031 Å away from the equatorial plane of the trigonal-bipyramidal co-ordination polyhedron, in which the C–Sn–S and C–Sn–C angles are all close to 120°; the O(1)–Sn–O(2^{I}) angle, 162.51(15)°, shows more distortion, probably because of the bite of the pyspa ligand and the role of O(2) in linking individual [SnEt$_2$(pyspa)] units.

The pyspa ligand. The quasi-planar pyspa ligand [the pyridine ring (r.m.s. = 0.0091) makes a dihedral angle of only 5.65° with the least-squares plane defined by Sn, S, O(1), C(1) and C(2) (r.m.s. = 0.0623)] is practically perpendicular (at 83.4°) to the equatorial plane of the co-ordination polyhedron, SnSC(11)C(21). The C(2)–S bond is slightly shorter than in other diorganotin(IV) thiolates[6,17] but close to the theoretical length of a single C–S bond, 1.81 Å.[18] The O(1)–C(1) and

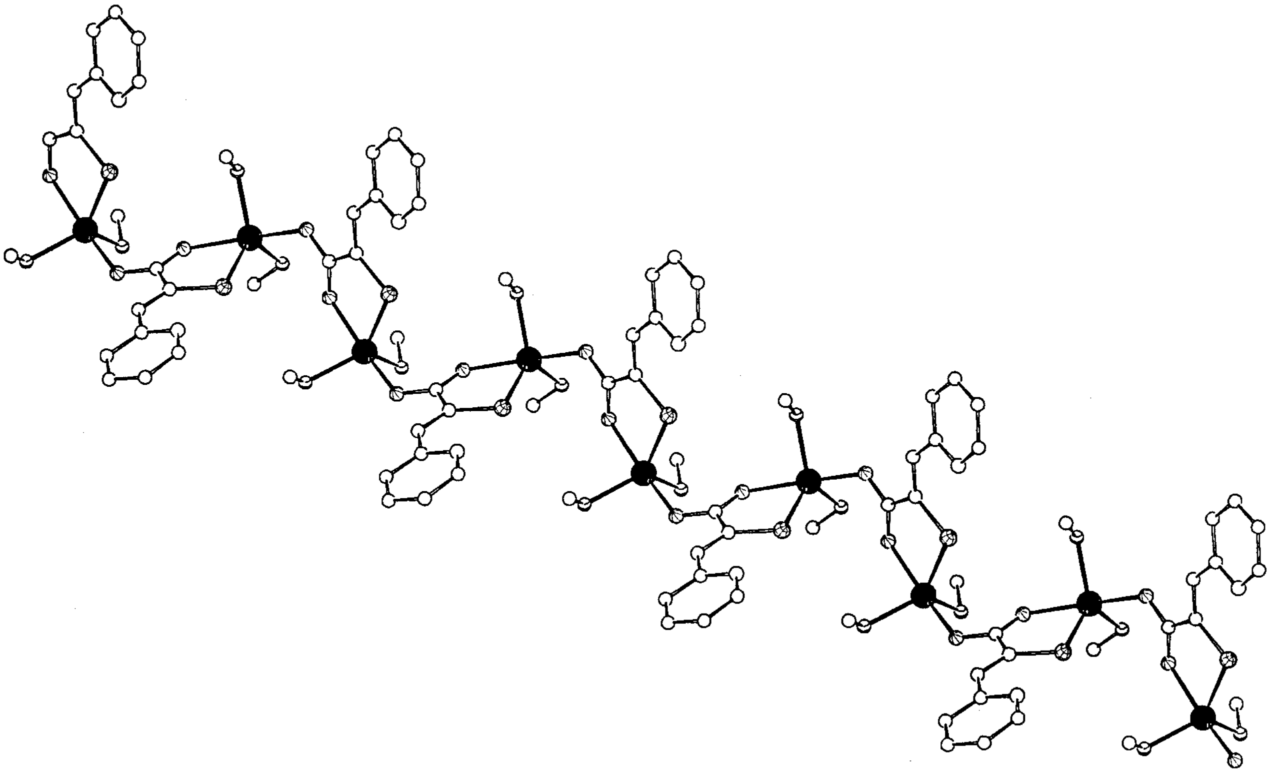

Fig. 2 Polymeric structure of [$SnEt_2$(pyspa)]

O(2)–C(1) bond lengths in the carboxylato group are similar to each other, in consonance with the similar Sn–O distances. The bridging behaviour of the ligand does not significantly widen the O–C–O angle.

Supramolecular association. The [$SnEt_2$(pyspa)] units are connected in a polymeric structure as shown in Fig. 2. Intermolecular tin–oxygen bonds [2.219(4)Å] that are comparable in strength to the intramolecular tin–oxygen bonds and close in length to the sum of the covalent radii of tin and oxygen, 2.13 Å,[16] create a continuous zigzag polymeric chain running along the *c* axis. The distance of 3.327 Å between Sn and O(1^I), though less than the sum of the van der Waals radii of tin and oxygen (3.70 Å),[16] is greater than in dibutyltin 3-sulfanylpropionate[5] and, as in that compound, the absence of any influence on the angles of the co-ordination polyhedron suggests that there is no significant interaction between these atoms.

The polymeric structure of [$SnEt_2$(pyspa)] recalls those of the carboxylates of type [$SnR_3(O_2CR')]_n$ reviewed by Tiekink,[19] with one R replaced by S in the equatorial plane, although [$SnEt_2$(pyspa)] has shorter intra- and inter-molecular Sn–O distances and a less linear O–Sn–O angle. Ng *et al.*[20] found that the repeat distance between alternate tin atoms in the [$SnR_3(O_2CR')]_n$ chain was virtually independent of both R and R′: increasing the size of these groups increased only the lengths of the other two axes of the unit cell, *i.e.* the distance between chains. The repeat Sn···Sn distance in the [$SnEt_2$(pyspa)]$_n$ chain, 5.155 Å, is close to the average of 5.185 Å in the seventeen triorganotin carboxylates studied by Ng *et al.*; this would suggest that diorganotin(IV) sulfanylcarboxylates which form polymeric chains comply with Ng *et al.*'s rule for triorganotin carboxylates, and hence that the unit-cell constants of diorganotin(IV) sulfanylcarboxylates may allow tentative prediction of whether the ligand co-ordinates *via* the sulfanylcarboxylato group or *via* some other donor group, and in the former case of whether the crystal consists of polymeric chains or not.[20] Crystallographic data for other sulfanylcarboxylato compounds would allow this suggestion to be tested.

Mössbauer spectra

The Mössbauer spectra of all the complexes at 80.0 K show a single quadrupole doublet with the parameters reported in the Experimental section. Clearly all three ligands form complexes with similar electronic properties and structural characteristics. The Mössbauer parameters depend almost exclusively on the R group of the SnR_2 moiety: the isomer shift varies with the inductivity and electronegativity of R, and the quadrupole splitting values are close to 3.17 mm s^{-1} for all nine alkyl derivatives and to 3.07 mm s^{-1} for all three phenyl complexes. Since calculations based on the point-charge model,[21] using published partial quadrupole splitting values and the bond angles determined for [$SnEt_2$(pyspa)], give a value of 3.29 mm s^{-1} for the alkyl derivatives and 2.93 mm s^{-1} for the phenyl compounds, in full agreement with the experimental results, it may be concluded that all the complexes have the same polymeric structure as that of [$SnEt_2$(pyspa)].

The above results, together with those reported for [SnR_2(L)] where R = alkyl or phenyl and L = $SCH_2CO_2^{2-}$[4e,21] or $S(CH_2)_2CO_2^{2-}$,[21] show that the benzene, pyridine and thiophene rings have little influence, if any, on the isomer shift and quadrupole splitting. They do, however, influence both the temperature dependence of the area of the resonant peaks and the ratio between the areas under the two peaks, $A_{2/1}$. In particular, for [$SnMe_2$(pspa)] the values of $A_{2/1}$ decrease steadily from 0.97 at 80.0 K to 0.85 at 200 K (Table 3), indicating the presence of a small Goldanski–Karyagin effect; this effect has been detected previously in only one compound of this type.[22] The linear dependence of the natural logarithm of the total resonance area on the temperature ($r = 0.979$) rules out a phase transformation, and the slope of the regression line, −0.011 35 K^{-1}, is lower than those reported for similar compounds and strongly supports the existence of a rigid polymeric structure[23] similar to that determined for [$SnEt_2$(pyspa)] by X-ray studies. Assuming that the whole [$SnMe_2$(pspa)] unit, with a molecular weight of 328, vibrates on absorbing the gamma photons, its Mössbauer temperature is 75.6 K.[22]

Table 3 Mössbauer effect parameters for [$SnMe_2$(pspa)] as a function of temperature

T/K	δ*/mm s^{-1}	ΔE_Q/mm s^{-1}	Γ/mm s^{-1}	$A_{2/1}$	ln A
80	1.35	3.16	0.87	0.97	0.0622
100	1.33	3.16	0.91	0.95	0.0584
120	1.37	3.18	0.90	0.93	0.0534
160	1.32	3.14	0.90	0.90	0.0295
200	1.33	3.12	0.86	0.85	0.0170

* Relative to room-temperature $CaSnO_3$.

Infrared and Raman spectra

To determine whether the vibrational bands of the complexes depended on the medium used,[24] the results obtained for KBr pellets were compared with those for Nujol (and in some cases Fluolube) mulls; no significant changes in the main bands were detected. The spectra of H_2tspa and H_2pspa showed bands typical of the SH group close to 2570 cm^{-1}, of medium-weak intensity in the IR spectrum and very weak in the Raman spectrum. In H_2pyspa the proton appears to have migrated to the pyridine N atom[25] (see below).

The vibrational patterns of the complexes have been analysed in the light of that of [$SnEt_2$(pyspa)], the structure of which was solved by X-ray diffraction. The carboxylato bands are similar for all the compounds. The $\Delta\nu$ values [$\nu_{asym}(CO_2^-) - \nu_{sym}(CO_2^-)$] range from 182 to 148 cm^{-1}; all are close to the 160 cm^{-1} found for [$SnEt_2$(pyspa)] and within the range generally accepted[4c,d,24,26] for bidentate bridging carboxylato groups. For the tspa and pspa complexes, the disappearance of the SH band of the free sulfanylcarboxylate and the presence of a new band around 350 cm^{-1} confirm co-ordination *via* S; for the pyspa complexes, the vibration near 350 cm^{-1} is also contributed to by a ligand band.

That all the complexes share the trigonal-bipyramidal co-ordination polyhedron found in [$SnEt_2$(pyspa)] is shown, in agreement with the Mössbauer data (see above), by their ν_{asym}(Sn–C) and ν_{sym}(Sn–C) vibrations, which in all cases indicate that the C–Sn–C fragment is non-linear.

NMR spectra

The ^1H and ^{13}C NMR data for the sulfanylcarboxylates and complexes are summarized in Tables 4–6. The very low solubility of the complexes in non-polar solvents obliged us to run the experiments in $(CD_3)_2SO$. Since H_2pspa and H_2pyspa rapidly degenerated in this solvent (as was shown by the appearance of sets of signals around δ 5.30 and 5.00 in the proton spectrum), the data were obtained with freshly prepared concentrated solutions. No degeneration of any of the tin complexes was detected under these conditions.

The apparent contradiction between the results obtained for H_2pyspa and those obtained for the other two ligands, together with the lack of published information on these compounds in this solvent (although ^1H and ^{13}C studies of H_2pspa in $CDCl_3$ and CD_3OD have been reported[27]), made it necessary to carry out DEPT and ^1H–^{13}C correlation experiments on the sulfanylcarboxylates and some complexes. These results, together with the published data,[27] allowed complete assignment of all the signals in the spectra of both the sulfanylcarboxylates and the tin compounds.

Assignment of the ^1H and ^{13}C signals of H_2pympa and its complexes was effected on the basis of the reported spectra of analogous compounds[27,28] and the ^1H–^{13}C cross-peaking of heteronuclear multiple quantum correlation (HMQC) and heteronuclear multiple bond correlation (HMBC) gradient-assisted spectra of H_2pyspa and [$SnEt_2$(pyspa)]. In the ^1H spectrum of H_2pyspa (Table 4) the presence of a broad singlet at δ 17.85 is coherent with protonation of the pyridine nitrogen, which together with the presence of only one proton on C(3) suggests that this compound is in the thione form in solution and not in the ene–thiol form like the other two (see below, ^{13}C data analysis, and ref. 27). Co-ordination to the diorganyltin species causes important changes in the ^1H spectrum. The very broad ligand signal attributed to C(1)OH does not appear for the complexes, and neither does the downfield N–H peak; reflecting deprotonation of both groups, evolution of the ligand to the thiol form and co-ordination of the metal through the carboxylato and thiol groups. The deshielding of C(3)H and the changes in the positions of the ring proton signals must be the result of deprotonation of the pyridine N and the change in the location of the double bonds (see Scheme 2).

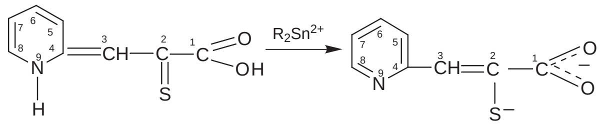

Scheme 2

The two peaks located at highest frequency in the ^{13}C NMR spectrum of H_2pyspa are attributed to C(1) and C(2). The latter is clearly deshielded with respect to its state in H_2pspa and H_2tspa (Tables 5 and 6), its signal lying in a position close to that found for compounds like 2-furanthiocarboxyhydrazide [H_3C_4O–C(S)–NH–NH_2][29] which is in the thione form. The ^{13}C NMR spectra of the pyspa complexes are all similar. The most significant features as regards the ligand are the slight deshielding of C(1), which reflects the monodentate character of the CO_2^- group[4e] and the disruption of the polymer existing in the solid state;[4e,5] the strong shielding of C(2) as a consequence of evolution to the thiol and co-ordination to the tin atom; and the shielding of C(3). The changes observed in the other carbon signals can also be attributed to the evolution to the thiol form, together with the deprotonation of the pyridine nitrogen.[30] The C(3)–Sn coupling indicated by two satellites flanking the C(3) signal of [$SnMe_2$(pyspa)] is indicative of co-ordination *via* S, while the satellites associated with the C(8) signal of [$SnEt_2$(pyspa)] may indicate the presence of species in which the pyridine nitrogen atom is co-ordinated.

In the ^1H NMR spectrum of H_2pspa (Table 5) the very broad signal located at δ 5.22 is attributed to the C(2)SH proton, while the one at δ 13.00 corresponds to the C(1)OH proton; neither of these signals appears in the spectra of the complexes, which is interpreted as due to the dideprotonation of the ligand. The other proton signals undergo only small changes in position. The most significant, that of C(5)H, can be associated with a change in the C(2)–C(3) bond order, since C(5)H is located in the deshielding cone of this bond. The influence of this bond may also explain why the C(3)H signal shifts so little upon complexation.

The ^{13}C NMR data show C(1) and C(2) to be only slightly deshielded in the pmpa complexes. Their signals lie not far away from the corresponding signals of the H_2pyspa compounds, which implies that both kinds of complex have the same kind of co-ordination. As in [$SnMe_2$(pyspa)], in [$SnMe_2$(pspa)] the shielding of C(3), and the satellites flanking its signal, add to the evidence of co-ordination *via* S.

All the above remarks concerning H_2pspa and its compounds may be generalized to H_2tspa, although the precise locations of the signals are of course slightly different.

The ^1H and ^{13}C chemical shifts and coupling constants of the organometallic moiety had very similar values for the compounds of all three ligands, which again suggests that all three have similar patterns of co-ordination. Finally, application of the Lockhart–Manders equations[31] to the $SnMe_2$ compounds predicted for all three ligands C–Sn–C angle values of about 130 (with the ^1H equation) or 125° (with the ^{13}C equation). Thus a trigonal-bipyramidal geometry with the methyl groups equatorial may be assumed for all these compounds, and the

Table 4 Proton and ^{13}C NMR data: pyspa compounds

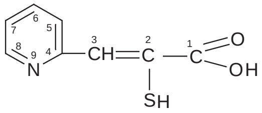

Sn-C(9)-C(10)-C(11)-C(12)

Compound	N(9)H	C(1)OH	C(2)SH	C(3)H	C(4)	C(5)H	C(6)H	C(7)H	C(8)H	RSn	$^nJ(^1H–Sn)$[a]	$^nJ(^{13}C–Sn)$[a]
H_2pyspa	17.85 (br s, 1)[b]	12.85 (vbr s, 1)	—	7.32 (s, 1)	—	7.70 (d, 1) [8.5][c]	8.15 (td, 1) [7.8][1.5]	7.51 (t, 1) [7.2]	8.53 (t, 1) [4.2]			
[SnMe$_2$(pyspa)]	—	—	—	7.77 (s, 1)	—	8.10 (d, 1) [8.0]	7.82 (td, 1) [7.7][1.7]	7.23 (dd, 1) [7.4]	8.61 (dd, 1) [4.4][0.7]	0.76 (s, 6)	79.7/78.0	
[SnEt$_2$(pyspa)]	—	—	—	7.74 (s, 1)	—	8.18 (d, 1) [7.9]	7.82 (td, 1) [7.7][1.7]	7.23 (dd, 1) [7.3][4.8]	8.61 (d, 1) [4.1]	1.42 (q, 4) H(9) 1.21 (t, 6) H(10)	131.2/125.5 69.8	
[SnBu$_2$(pyspa)]	—	—	—	7.75 (s, 1)	—	8.12 (d, 1) [7.9]	7.82 (td, 1) [7.9][1.7]	7.24 (dd, 1) [7.3][4.3]	8.62 (d, 1) [4.2]	1.55 (m, 4) H(10) 1.42 (m, 4) H(9) 1.32 (m. 4) H(11) 0.85 (t, 6) H(12)		
[SnPh$_2$(pyspa)]	—	—	—	7.89 (s, 1)	—	7.97 (d, 1) [7.8]	7.85 (td, 1) [7.7]	7.28 (t, 1) [6.1]	8.67 (d, 1) [4.2]	7.69 (d. 4) H_o 7.50 (m. 6) H_m, H_p		
H_2pyspa	—	167.6	167.8	113.1	151.7	126.2	142.1	121.0	135.7			
[SnMe$_2$(pyspa)]	—	168.5	136.1	131.6 [26.7]	155.2	124.0	135.1	121.8	149.3	4.0		626.7/598.9
[SnEt$_2$(pyspa)]	—	169.1	135.8	131.6	155.3	123.9	136.1	121.8	149.3 [215.2]	15.8 C(9) 9.6 C(10)		610.7/583.4 43.0
[SnBu$_2$(pyspa)]	—	168.7	136.1	131.7	155.2	124.0	135.3	121.8	149.3	27.0 C(10) 25.7 C(9) 22.5 C(11) 13.5 C(12)		36.8
[SnPh$_2$(pyspa)]	—	168.0	136.4	132.4	154.6	124.8	136.8	122.2	149.2	140.2 C_i 135.5 C_o 130.2 C_p 129.0 C_m		 54.2

[a] Coupling constants, $^1H–^{119/117}Sn$ and $^{13}C–^{119/117}Sn$, in Hz. [b] Relative number of protons. [c] Other coupling constants.

Table 5 Proton and ^{13}C NMR data: pspa compounds

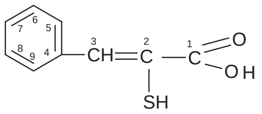

Sn-C(10)-C(11)-C(12)-C(13)

Compound	C(1)OH	C(2)SH	C(3)H	C(4)	$C(5)H_o$	$C(6)H_m$	$C(7)H_p$	RSn	$^nJ(^1H–Sn)$	$^nJ(^{13}C–Sn)^a$
H_2pspa	13.0 (vbr)	5.22 (vbr)	7.73 (s, 1)	—	7.68 (d, 2) [7.6]	7.47 (t)	7.39 (m)			
$[SnMe_2(pspa)]$	—	—	7.69 (s, 1)	—	7.90 (d, 2) [7.5]	7.41 (t, 2) [7.5]	7.28 (t, 1) [7.3]	0.76 (s, 6)	80.0	
$[SnEt_2(pspa)]$	—	—	7.67 (s, 1)	—	7.92 (d, 2) [7.3]	7.40 (t, 2) [7.3]	7.27 (t. 1) [7.4]	1.40 (q, 4) H(10) 1.21 (t, 6) H(11)	131.2/125.6 70.0	
$[SnBu_2(pspa)]$	—	—	7.68 (s, 1)	—	7.91 (d, 2) [7.7]	7.41 (t, 2) [7.5]	7.28 (t, 1) [7.4]	1.55 (m, 4) H(11) 1.41 (m, 4) H(10) 1.32 (m, 4) H(12) 0.85 (t, 6) H(13)		
$[SnPh_2(pspa)]$	—	—	7.84 (s, 1)	—	7.93 (d, 2) [7.5]	7.44 (t, 2) [7.6]	7.32 (t, 1) [7.4]	7.69 (d, 4) H_o 7.49 (t, 6) H_m, H_p		
H_2pspa	167.1	129.5	145.6	134.4	131.3	129.4	130.8			
$[SnMe_2(pspa)]$	168.8	129.5	131.6 [28.7]	136.5	129.5	128.2	127.7	4.0		627.7/600.0
$[SnEt_2(pspa)]$	169.4	131.7	131.3	136.7	128.2	129.5	127.4	15.7 C(10) 9.3 C(11)		622.6/599.3 43.6
$[SnBu_2(pspa)]$	169.1	131.5	131.1	136.5	128.2	129.5	127.6	27.0 C(11) 25.7 C(10) 22.5 C(12) 13.5 C(13)		
$[SnPh_2(pspa)]$	168.4	133.0	130.4	136.1	128.4	129.6	128.1	140.1 C_i 135.5 C_o 129.2 C_p 129.1 C_m		 60.4

Table 6 Proton and ^{13}C NMR data: tspa compounds

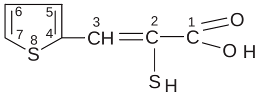

Sn-C(8)-C(9)-C(10)-C(11)

Compound	C(1)OH	C(2)SH	C(3)H	C(4)	C(5)H	C(6)H	C(7)	RSn	$^nJ(^1H–Sn)$	$^nJ(^{13}C–Sn)$
H_2tspa	12.82 (br s, 1)	—	8.17 (s, 1)	—	7.57 (d, 1) [3.2]	7.08 (st, 1) [4.9] [3.9]	7.77 (d. 1) [5.9]			
[SnMe$_2$(tspa)]	—	—	7.93 (s, 1)	—	7.43 (d, 1) [3.3]	7.13 (dd, 1) [3.7] [5.0]	7.65 (dd, 1) [5.0]	0.78 (s, 6)	81.4/78.7	
[SnEt$_2$(tspa)]	—	—	7.91 (s, 1)	—	7.43 (d, 1) [3.3]	7.13 (dd, 1) [3.7] [5.0]	7.63 (dd, 1) [4.2]	1.42 (q, 4) H(8) 1.20 (t, 6) H(9)	133.6/127.8 70.7	
[SnBu$_2$(tspa)]	—	—	7.92 (s, 1)	—	7.43 (d, 1) [3.2]	7.13 (dd, 1) [5.1] [3.7]	7.64 (dd, 1) [4.2]	1.56 (m, 4) H(9) 1.44 (m, 4) H(8) 1.32 (m, 4) H(10) 0.85 (t, 6) H(11)		
[SnPh$_2$(tspa)]	—	—	8.09 (s, 1)	—	7.50*	7.17 (dd, 1) [5.1] [3.7]	7.73*	7.69* H_o 7.49* H_m, H_p	74.7	
H_2tspa	166.2	123.1	140.4	137.3	137.7	127.2	134.2	—		
[SnMe$_2$(tspa)]	168.7	128.8	125.2 [31.8]	140.9	130.2	126.9	127.7	4.6		637.3/609.0
[SnEt$_2$(tspa)]	169.3	129.5	125.1	141.0	130.1	126.8	127.5	16.5 C(8)		
								9.6 C(9)		44.8
[SnBu$_2$(tspa)]	169.0	128.8	125.4	140.9	130.3	126.9	127.7	25.7 C(8)		36.3
								27.0 C(9)		
								23.0 C(10)		
								13.5 C(11)		
[SnPh$_2$(tspa)]	168.3	126.7	126.6	140.2	131.2	127.2	128.6	140.3 C_i		
								135.5 C_o		55.1
								130.4 C_p		17.2
								129.0 C_m		81.9

st = Pseudo-triplet. * Overlapping the SnPh$_2$ signals.

same is probably true of the other complexes. This shows that the break-up of the solid-state polymer does not significantly alter the environment of the tin atom, which suggests the co-ordination of a $(CD_3)_2SO$ molecule instead of the neighbouring $[SnR_2L]$ unit that in the solid state is co-ordinated *via* its O(2) atom.

References

1 C. J. Evans, in *The Chemistry of Tin*, ed. P. G. Harrison, Chapman and Hall, New York, 1989, p. 421; M. T. Musmeci, G. Madonia, M. T. Lo Giudice, A. Silvestri, G. Ruissi and R. Barbieri, *Appl. Organomet. Chem.*, 1992, **6**, 127.

2 A. Barbieri, A. M. Giuliani, G. Ruissi, A. Silvestri and R. Barbieri, *Z. Anorg. Allg. Chem.*, 1995, **621**, 89.

3 R. D. Deanin and S. R. Deshmukh, *Polym. Mater. Sci. Eng.*, 1995, **73**, 479.

4 (*a*) G. Domazetis, M. F. Mackay, R. J. Magee and B. D. James, *Inorg. Chim. Acta*, 1979, **34**, L247; (*b*) J. D. Cashion, G. Domazetis and B. D. James, *J. Organomet. Chem.*, 1980, **185**, 433; (*c*) G. K. Sharma and N. Sharma, *Appl. Organomet. Chem.*, 1993, **7**, 33 and refs. therein; (*d*) C. D. Hager, F. Huber, A. Silvestri, A. Barbieri and R. Barbieri, *Gazz. Chim. Ital.*, 1993, **123**, 583; (*e*) K. Gajda-Schrantz, L. Nagy, E. Kuzmann, A. Vértes, J. Holecek and A. Lycka, *J. Chem. Soc.*, *Dalton Trans.*, 1997, 2201.

5 T. P. Lockhart, *Organometallics*, 1988, **7**, 1438.

6 J. Meunier-Piret, M. Boualam, R. Willem and M. Gielen, *Main Group Met. Chem.*, 1993, **16**, 329.

7 A. Izquierdo and J. L. Beltrán, *Mikrochim. Acta* (*Wien*) *II*, 1989, 91 and refs. therein.

8 E. Campaigne and R. E. Cline, *J. Am. Chem. Soc.*, 1956, **21**, 32.

9 B. A. Frenz, in *Computing in Crystallography*, eds. H. Schenk, R. Olthof-Hazekamp, H. Van Koningsveld and G. C. Bassi, Delft University Press, 1985, vol. 2.2, pp. 64–71.

10 N. Walker and D. Stuart, *Acta Crystallogr.*, *Sect. A*, 1983, **39**, 158.

11 G. M. Sheldrick, *Acta Crystallogr.*, *Sect. A*, 1990, **46**, 467.

12 G. M. Sheldrick, SHELXL 97. Program for the refinement of crystal structures. University of Göttingen, 1997.

13 *International Tables for X-Ray Crystallography*, Kynoch Press, Birmingham, 1984, vol. 4 (Present distributor Kluwer Academic Publishers, Dordrecht).

14 L. Zsolnai, ZORTEP, A program for the presentation of thermal ellipsoids, University of Heidelberg, 1997.

15 E. Keller, SCHAKAL, A program for plotting molecular and crystal structures, University of Freiburg, 1988.

16 E. J. Huheey, E. A. Keiter and R. L. Keiter, *Inorganic Chemistry. Principles of Structure and Reactivity*, Harper Collins College Publishers, New York, 4th edn., 1993, p. 292.

17 M. V. Castaño, A. Macías, A. Castiñeiras, A. Sánchez González, E. García Martinez, J. S. Casas, J. Sordo, W. Hiller and E. E. Castellano, *J. Chem. Soc.*, *Dalton Trans.*, 1990, 1001.

18 J. D. Curry and R. J. Jandecek, *J. Chem. Soc.*, *Dalton Trans.*, 1972, 1120.

19 E. R. T. Tiekink, *Appl. Organomet. Chem.*, 1991, **5**, 1.

20 S. W. Ng, Ch. Wei and V. G. Kumar Das, *J. Organomet. Chem.*, 1988, **345**, 59.

21 R. V. Parish, in *Mössbauer Spectroscopy Applied to Inorganic Chemistry*, ed. G. J. Long, Plenum, New York, 1994, vol. 1, ch. 16.

22 R. Barbieri, A. Silvestri, A. Barbieri, G. Riusi, F. Huber and C. D. Hager, *Gazz. Chim. Ital.*, 1994, **124**, 187.

23 K. C. Molloy and K. Quill, *J. Chem. Soc.*, *Dalton Trans.*, 1985, 1417.

24 G. B. Deacon and R. Phillips, *Coord. Chem. Rev.*, 1980, **33**, 227.

25 D. Cook, *Can. J. Chem.*, 1961, **39**, 2009.

26 K. Nakamoto, *Infrared and Raman Spectra of Inorganic and Coordination Compounds*, Wiley, New York, 4th edn., 1986, p. 231.

27 H. H. Lee, A. Kuwae and K. Hanai, *Spectrosc. Lett.*, 1984, **27**, 787.

28 M. Danish, G. H. Alt, A. Badshah, S. Ali, M. Mazhar and N. Islam, *J. Organomet. Chem.*, 1995, **468**, 51.

29 J. S. Casas, A. Castiñeiras, A. Macias, M. C. Rodriguez Argüelles, A. Sánchez and J. Sordo, *Inorg. Chim. Acta*, 1992, **197**, 163.

30 R. Haran, F. Nepven-Juras and J. P. Laurent, *Org. Magn. Reson.*, 1977, **10**, 203.

31 T. P. Lockhart and W. F. Manders, *Inorg. Chem.*, 1986, **25**, 892.

Received 14*th November* 1997; *Paper* 7/08202I